Check for updates

MoChlo: A Versatile, Modular Cloning Toolbox for Chloroplast Biotechnology[1][OPEN]

Alessandro Occhialini,[a,b,2] Agnieszka A. Piatek,[c,2] Alexander C. Pfotenhauer,[a,b] Taylor P. Frazier,[b,c,d] C. Neal Stewart Jr.,[b,c] and Scott C. Lenaghan[a,b,3,4]

[a]Department of Food Science, University of Tennessee, Knoxville, Tennessee 37996
[b]Center for Agricultural Synthetic Biology, Institute of Agriculture, University of Tennessee, Knoxville, Tennessee 37996
[c]Department of Plant Sciences, University of Tennessee, Knoxville, Tennessee 37996
[d]Elo Life Systems, Durham, North Carolina 27709

ORCID IDs: 0000-0002-1162-798X (A.O.); 0000-0003-3026-9193 (C.N.S.); 0000-0002-7539-1726 (S.C.L.).

Plant synthetic biology is a rapidly evolving field with new tools constantly emerging to drive innovation. Of particular interest is the application of synthetic biology to chloroplast biotechnology to generate plants capable of producing new metabolites, vaccines, biofuels, and high-value chemicals. Progress made in the assembly of large DNA molecules, composing multiple transcriptional units, has significantly aided in the ability to rapidly construct novel vectors for genetic engineering. In particular, Golden Gate assembly has provided a facile molecular tool for standardized assembly of synthetic genetic elements into larger DNA constructs. In this work, a complete modular chloroplast cloning system, MoChlo, was developed and validated for fast and flexible chloroplast engineering in plants. A library of 128 standardized chloroplast-specific parts (47 promoters, 38 5′ untranslated regions [5′UTRs], nine promoter:5′UTR fusions, 10 3′UTRs, 14 genes of interest, and 10 chloroplast-specific destination vectors) were mined from the literature and modified for use in MoChlo assembly, along with chloroplast-specific destination vectors. The strategy was validated by assembling synthetic operons of various sizes and determining the efficiency of assembly. This method was successfully used to generate chloroplast transformation vectors containing up to seven transcriptional units in a single vector (~10.6-kb synthetic operon). To enable researchers with limited resources to engage in chloroplast biotechnology, and to accelerate progress in the field, the entire kit, as described, is available through Addgene at minimal cost. Thus, the MoChlo kit represents a valuable tool for fast and flexible design of heterologous metabolic pathways for plastid metabolic engineering.

The plastids of land plants represent an underutilized resource with regard to metabolic engineering of heterologous pathways (Maliga and Bock, 2011; Bock, 2013; Jin and Daniell, 2015; Schindel et al., 2018). Plastids have been successfully engineered for expression of valuable carotenoids (Wurbs et al., 2007; Apel and Bock, 2009) and terpenoids (Pasoreck et al., 2016) as well as for the production of numerous biopharmaceuticals (Davoodi-Semiromi et al., 2010; Boyhan and Daniell, 2011; Lakshmi et al., 2013). Nonetheless, there are far fewer instances in which the plastid chassis has been engineered for crop improvement traits. Certainly, a more controlled metabolic engineering approach would facilitate a fundamental change in crop improvement (Schindel et al., 2018). One such example, using plastid engineering, is the metabolic engineering of a complete carbon-concentrating mechanism from cyanobacterium into plastids for improving photosynthesis (Lin et al., 2014a, 2014b; Occhialini et al., 2016; Long et al., 2018). Since plastid genomes are relatively conserved among land plants, improving photosynthesis in one species via plastids should be translatable to other species (McNeal et al., 2007).

There are several advantages to engineering plastid genomes, as opposed to nuclear ones, for metabolic engineering in plants. Plastids have small genomes (120–217 kb) present in multiple copies (e.g. ~10,000 plastome copies per cell in tobacco [*Nicotiana tabacum*]), lack gene-silencing machinery, and are capable of extremely high levels of foreign protein production (10%–70% total soluble protein). Also, transgene insertion is achieved through homologous recombination, providing a known landing site for insertion

[1]This work was supported by the Advanced Research Projects Agency-Energy (award no. DE-AR000660), USDA Hatch Grants (accession no. 1012962 and 1016740), and the Defense Advanced Research Projects Agency (award no. D17AC00016).

[2]These authors contributed equally to the article.

[3]Author for contact: slenagha@utk.edu.

[4]Senior author.

The author responsible for distribution of materials integral to the findings presented in this article in accordance with the policy described in the Instructions for Authors (www.plantphysiol.org) is: Scott C. Lenaghan (slenagha@utk.edu).

S.C.L., A.P., and A.O. designed the strategy and compiled the sequences; A.O., A.C.P., and T.P.F. collected and analyzed data; A.O., C.N.S., and S.C.L. wrote the article.

[OPEN]Articles can be viewed without a subscription.

www.plantphysiol.org/cgi/doi/10.1104/pp.18.01220

 © 2019 American Society of Plant Biologists. All Rights Reserved.

(Kuroda and Maliga, 2001a; Maliga, 2004; Shaver et al., 2006; Verma and Daniell, 2007; Verma et al., 2008; Oey et al., 2009a; Schelkunov et al., 2015). Furthermore, since chloroplasts are prokaryotic in origin, the transcription and translation machinery functions similar to prokaryotes, allowing for coordinated gene expression in operons (Bock, 2013; Lu et al., 2013). For metabolic engineering, the ability to coordinate the expression of multiple genes is essential for controlling complex multigene pathways. Unfortunately, while the regulatory machinery of plastids is prokaryotic in origin, the governing rules/functional motifs used for gene expression are not nearly as well characterized as their bacterial counterparts. Thus, while numerous logic circuits and tunable expression systems have been developed in bacterial systems, few exist for plastids (Verhounig et al., 2010; Emadpour et al., 2015). Instead, most complex pathways expressed in plastids use a single promoter to drive equivalent expression of all transgenes in the pathway (Lu et al., 2013; Fuentes et al., 2016). However, excess production of heterologous protein, even green fluorescent protein (GFP), has had demonstrable negative effects on chloroplast metabolic function and the overall phenotype of the resulting plants (Oey et al., 2009a). Advanced metabolic engineering in plastids requires an understanding of how to tune the stoichiometry of multiple genes within a heterologous pathway to achieve the desired product (Bock, 2013, 2015; Schindel et al., 2018).

Typically, heterologous genes engineered into plastids are placed under the control of endogenous regulatory sequences (Tregoning et al., 2003; Lutz et al., 2007; Zhou et al., 2008; Oey et al., 2009b). For effective chloroplast metabolic engineering with tunable expression, the following components must be considered: promoters, 5′ untranslated regions (5′UTRs), and 3′UTRs. Precise regulation of gene expression in plastids could be controlled by varying these components to achieve the desired expression level for each transgene or operon. While combinatorial and permutational analyses of these components in a bacterial chassis, such as *Escherichia coli*, are routinely conducted, plastids represent a more challenging system because the plastid toolkit is much less developed than that for bacteria. In addition, compared with nuclear engineering in plants, few labs currently conduct plastid engineering.

In this article, we describe a plastid molecular cloning kit, MoChlo, for plastid genetic engineering in plants. The MoChlo kit builds on previously developed modular cloning kits (Sarrion-Perdigones et al., 2011; Weber et al., 2011; Lampropoulos et al., 2013; Engler et al., 2014; Vafaee et al., 2014). Our goals are to lower the barrier of entry into plastid engineering, to enable troubleshooting for transgene expression, and to provide more flexibility for plastid metabolic engineering. Our hope is that a standardized assembly kit composed of a library of plastid regulatory elements will accelerate research into metabolic engineering in plastids and benefit the research community as a whole.

RESULTS

MoChlo Kit Design

The nomenclature and strategy used for the various levels and components of the MoChlo system were adopted from previous plant MoClo kits (Fig. 1; Supplemental Fig. S1; Weber et al., 2011; Engler et al., 2014). All individual parts (Level-0) mined from the literature were domesticated using the criteria described in "Materials and Methods." The domesticated MoChlo parts library comprises 47 chloroplast promoters, 38 5′UTRs, nine fused chloroplast promoter::5′UTRs, and 10 terminators/3′UTRs. In addition, the library includes 14 coding genes including selectable markers (e.g. *aadA*) and reporter genes (e.g. *mEmerald* GFP). A complete list of all Level-0 modules provided in the MoChlo kit, including references to where the sequence was mined, is shown in Table 1 and Supplemental Table S1. All 14 Level-1 destination vectors (seven in forward and seven in reverse orientation) were obtained directly from a previous MoClo kit (Engler et al., 2014; Supplemental Table S2). With the current components of the MoChlo kit, it is possible to assemble up to seven Level-1 constructs into a single Level-2 construct (Fig. 1; Supplemental Fig. S2). In addition, a set of seven end linkers compatible with the 3′ overhang of each position of the final operon provides the option to integrate a variable number of cassettes into Level-2 vectors (Supplemental Fig. S2; Supplemental Table S3). The final components of the MoChlo system are the Level-2 chloroplast-specific destination vectors. The Level-2 destination vectors in the MoChlo system were developed for three plant species (tobacco, maize [*Zea mays*], and potato [*Solanum tuberosum*]) with homologous arms designed for recombination into four different integration sites of the plastome (*trnI-trnA*, *trnG-trnfM*, *trnV-3′rps12*, and *atpB-accD*; Supplemental Table S3). Thus, in the current version of the MoChlo kit, researchers would be able to directly assemble chloroplast transformation cassettes for multiple plant species utilizing a variety of regulatory elements as well as selectable marker genes.

Validation of the MoChlo Strategy for Assembly of Simple Synthetic Operons (Four or Fewer Transcriptional Units)

The first step in validating the MoChlo kit was assembling Level-1 constructs from the Level-0 parts (Fig. 2). Four Level-1 transcriptional units expressing *GOI-1*, *GOI-2*, *GOI-3*, or *aadA* were cloned into four Level-1 vectors for positions 1, 2, 3, and 4 of the operon, respectively. A description of regulatory sequences (Level-0 parts) used to assemble the aforementioned 1A, 1B, 1C, and 1D Level-1 cassette is shown in Table 2. The efficiency of assembly of the Level-1 constructs was 100%, as determined by blue-white screening, PCR, and restriction digestion (Fig. 2; Supplemental Fig. S3). Finally, the correct nucleotide sequence of all Level-1 constructs was verified by Sanger sequencing.

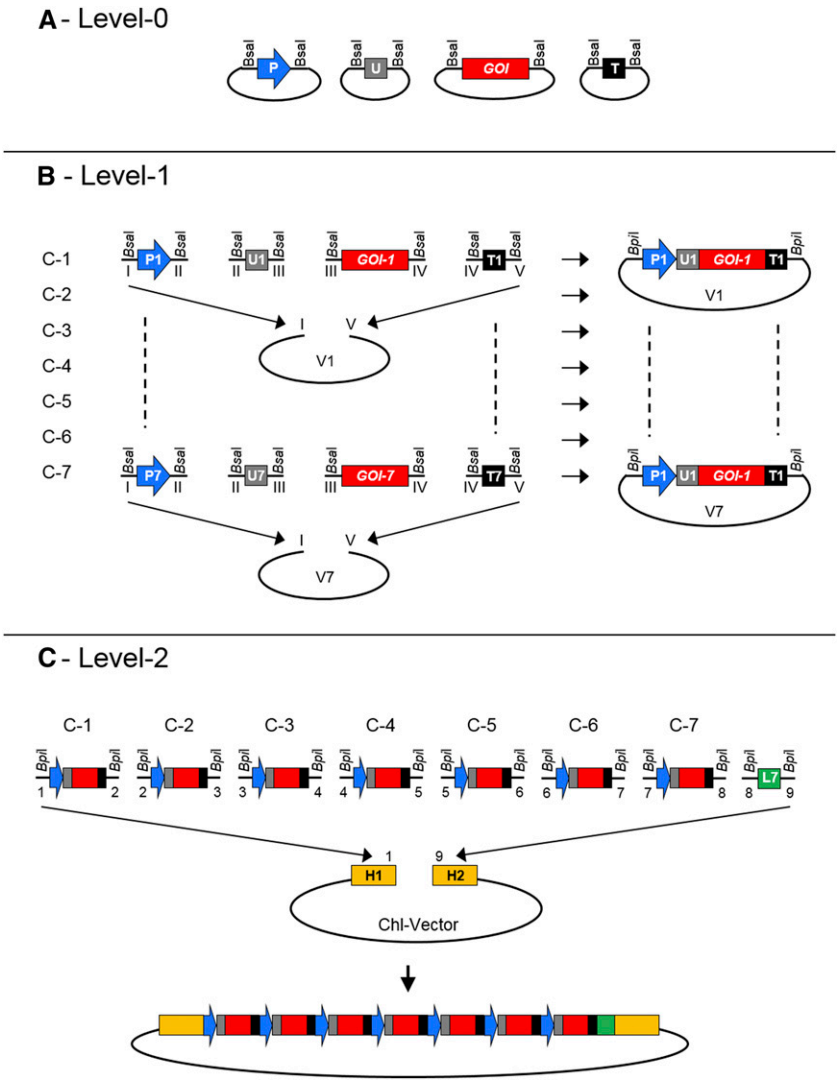

Figure 1. Schematic representation of Golden Gate assembly using the MoChlo kit. A, Four vectors containing different Level-0 modules flanked by *Bsa*I sites. P, Promoter (blue); U, 5′UTR (gray); GOI, gene of interest (red); T, terminator/3′UTR (black). B, Level-1 Golden Gate assembly. The *Bsa*I restriction digestion releases Level-0 parts (P1–P7, U1–U7, GOI1–GOI7, and T1–T7) equipped with 5′ and 3′ overhangs (I–V) used for directional cloning. The 5′ and 3′ overhangs (I and V, respectively) of P-U-GOI-T cassettes (C1–C7) are compatible with Level-1 vectors (V1–V7). The Level-1 assembly results in seven Level-1 vectors containing seven cassettes (C1–C7) flanked by *Bpi*I sites. C, Level-2 Golden Gate assembly. The *Bpi*I restriction digestion of Level-1 vectors releases cassettes (C1–C7) equipped with 5′ and 3′ overhangs (1–8) able to provide directional cloning from C1 to C7. An end linker (L7; green) equipped with compatible 5′ and 3′ overhangs (8 and 9, respectively) allows integration of the Level-2 operon in between the homologous sequences (H1 and H2) of a chloroplast transformation vector (Chl-Vector; destination vector Level-2).

Examples of another 14 Level-1 cassettes assembled using the MoChlo kit are shown in Supplemental Figure S4 and had the same efficiency of 100%.

To validate Level-2 assembly, Level-2 operon-1 (~3.5 kb) was assembled in a second assembly step using the four Level-1 cassettes (1A, 1B, 1C, and 1D) generated previously. For this assembly, a Level-2 destination vector equipped with homologous arms to *trnG-trnfM* from potato was used (Fig. 3). This operon was designed to represent a standard polycistronic operon (three GOI) along with a monocistronic selection cassette. Using *Bbs*I to release all of the Level-1 cassettes for Level-2 assembly, the efficiency of Level-2 assembly, as determined by PCR, was 22.5% (Supplemental Fig. S5). However, when using the isoschizomer *Bpi*I instead, GOI-1 was found to be present in all 40 colonies tested, with 37 of the colonies positive for all genes in the cassette (Supplemental Fig. S6). Thus, the efficiency of Level-2 assembly was 92.5% using *Bpi*I instead of *Bbs*I, as determined by colony PCR. With a simpler assembly combining only two Level-1 cassettes into Level-2, instead of the four described previously, there was no difference in efficiency between assembly using *Bbs*I and *Bpi*I, with both achieving 100% efficiency (Supplemental Fig. S7). Correct assembly of Level-2 operon-1 was further verified by PCR of the individual components (Fig. 3) as well as by PCR confirmation of the junctions between individual Level-1 constructs (*trnG/GOI-1*, *GOI-1/GOI-2*, *GOI-2/GOI-3*, *GOI-3/aadA*, and *aadA/trnfM*; Fig. 3). Examples of another four Level-2 operons assembled by the same four Level-1 cassettes are shown in Supplemental Figure S8.

Validation of MoChlo Strategy for Assembly of a Large Operon (Seven Transcriptional Units)

In the current iteration of the MoChlo kit, the maximum number of Level-1 constructs that can be combined into a single Level-2 cassette is seven. To test the efficiency of the maximum assembly, the six genes

Table 1. *Level-0 parts provided in the MoChlo kit*

A detailed description of all Level-0 parts, including nucleotide sequences, is included in Supplemental Table S1. (–), No data; u, unpublished; NEP, nuclear encoded polymerase; PEP, plastid encoded polymerase; DB, downstream box; Ec, Escherichia coli; TYMV, turnip yellow mosaic virus; BMV, brome mosaic virus; AMV, Alfalfa mosaic virus; TMV, tobacco mosaic virus; SL, stem-loop; codon opt., plastid codon optimized.

Promoters		5′UTR	
P*accD* (−82 to +23; Hirata et al., 2004)	P*rrn16* (Allison et al., 1996)	*atpB* 5′UTR (Hirose and Sugiura, 2004)	*rbcL* 5′UTR (full; Yukawa et al., 2007)
P*accD* (functional; Hirata et al., 2004)	P*rrn* (tobacco; Suzuki et al., 2003)	*atpB* 5′UTR +10 (functional; Hirose and Sugiura, 2004)	*rbcL* 5′UTR (processed; Yukawa et al., 2007)
P*atpB* (NEP functional PEP disabled; Xie and Allison, 2002)	Synthetic AP*rrn1*^{u}	*atpB* 5′UTR +10 processed −90 (functional; Yukawa et al., 2007)	*rbcL* 5′UTR + 14 AA (Kuroda and Maliga, 2001b)
P*atpB* (NEP; Xie and Allison, 2002)	Synthetic AP*rrn2*^{u}	*atpB* 5′UTR TCR processed −90 (functional; Kuroda and Maliga, 2001b)	Synthetic RBS (Kuroda and Maliga, 2001a)
P*atpB* (PEP and NEP functional; Xie and Allison, 2002)	Synthetic AP*rrn3*^{u}	*atpH* 5′UTR (Yukawa et al., 2007)	T7G10 leader (Kuroda and Maliga, 2001a)
P*atpB* (PEP functional NEP disabled; Xie and Allison, 2002)	Synthetic AP*rrn4*^{u}	*atpH* 5′UTR processed −45 (Yukawa et al., 2007)	T7G10 leader + Ec DB (Kuroda and Maliga, 2001a)
P*atpB* (PEP; Xie and Allison, 2002)	Synthetic AP*rrn5*^{u}	*atpI* 5′UTR (Baecker et al., 2009)	*rrn16* 5′UTR (native; Allison et al., 1996)
P*atpH* (Miyagi et al., 1998)	Synthetic AP*rrn6*^{u}	*psbN* 5′UTR (Kuroda and Sugiura, 2014)	*rrn16* 5′UTR (+37; Allison et al., 1996)
P*atpI* (NEP; Miyagi et al., 1998)	Synthetic AP*rrn7*^{u}	*psbN* 5′UTR processed −39 (Kuroda and Sugiura, 2014)	*psbA* 5′UTR (Staub and Maliga, 1994)
P*atpI* (PEP hypothetical; Miyagi et al., 1998)	Synthetic AP*rrn8*^{u}	*psbB* 5′UTR (Yukawa et al., 2007)	Synthetic RBS (Allison and Maliga, 1995)
P*clpP* (Sriraman et al., 1998)	Synthetic AP*rrn9*^{u}	*psbB* 5′UTR processed −54 (Yukawa et al., 2007)	*psbC* 5′UTR (Kuroda et al., 2007)
P*clpP* (PEP; Sriraman et al., 1998)	Synthetic AP*rrn10*^{u}	*ndhD* 5′UTR (Hirose and Sugiura, 1996)	*accD* 5′UTR (Caroca et al., 2013)
IEE (Zhou et al., 2007)	Synthetic BP*rrn12*^{u}	*rps2* 5′UTR (Plader and Sugiura, 2003)	*clpP* 5′UTR (Kuroda and Maliga, 2002)
P*rrn* (−64 to +17; Suzuki et al., 2003)	Synthetic BP*rrn13*^{u}	*rps2* 5′UTR mAAGA (Plader and Sugiura, 2003)	–
mP*rrn* (5-fold decrease transcription; Suzuki et al., 2003)	Synthetic BP*rrn14*^{u}	*rps2* 5′UTR mCCUC (Plader and Sugiura, 2003)	–
P*psbA* (Staub and Maliga, 1994)	Synthetic BP*rrn15*^{u}	*rps2* 5′UTR mAAGA (−20 to −10 deletion; Plader and Sugiura, 2003)	–
P*psbA* (−42 to +9; Hayashi et al., 2003)	Synthetic BP*rrn16*^{u}	*rps2* 5′UTR mCCUC (−20 to −10 deletion; Plader and Sugiura, 2003)	–
P*psbB* (Tanaka et al., 1987)	Synthetic BP*rrn17*^{u}	*psbH* 5′UTR + start codon + 1 AA (Hammani et al., 2012)	–
P*psbD* leader (Allison and Maliga, 1995)	Synthetic BP*rrn18*^{u}	*psbA* 5′UTR (SNM; Zou et al., 2003)	–
P*psbD*-PGTbx (Allison and Maliga, 1995)	Synthetic BP*rrn19*^{u}	*psbA* 5′UTR (SEM; Zou et al., 2003)	–
P*psbD* (Allison and Maliga, 1995)	Synthetic BP*rrn20*^{u}	*psbA* 5′UTR (delta SL; Zou et al., 2003)	–
P*rbcL* (Shiina et al., 1998)	Synthetic BP*rrn21*^{u}	*psbA* 5′UTR (delta 5′SL; Zou et al., 2003)	–
P*rbcL* (core −3 to +9; Shiina et al., 1998)	–	*psbA-rbcL* chimeric 5′UTR (R delta 5′SL; Zou et al., 2003)	–
P*rbcL* (−110 to +9; Shiina et al., 1998)	–	*psbA-rbcL* chimeric 5′UTR (R′SLWT; Zou et al., 2003)	–
P*rpoB* (Liere and Maliga, 1999)	–	*rps14* 5′UTR (Hirose et al., 1998)	–

Promoter::5′UTR	GOI	Integration Sites	3′UTR
Maize P*clpP*::5′UTR (Zhang et al., 2012)	*mEmerald* (Cubitt et al., 1999)	Tobacco *trnI/trnA* (Daniell et al., 1998)	*psbA* 3′UTR (Eibl et al., 1999)
Maize P*clpP*::Gg10 leader (Zhang et al., 2012)	*pporRFP* (Alieva et al., 2008)	Tobacco *trnG/trnfM* (Bock and Maliga, 1995)	*rbcL* 3′UTR (Eibl et al., 1999)
P*accD*::5′UTR (Zhang et al., 2012)	*aadA* (Svab and Maliga, 1993)	Tobacco *trnV/3′rps12* (Staub and Maliga, 1992)	*petD* 3′UTR (Tangphatsornruang et al., 2011)
mP*rrn*::RBS (3.9%; Suzuki et al., 2003)	*aphA6* (Huang et al., 2002)	Tobacco *atpB/accD* (Lin et al., 2014b)	*rpoA* 3′UTR (Tangphatsornruang et al., 2011)
mP*rrn*::RBS (20%; Suzuki et al., 2003)	*nptII* (Carrer et al., 1993)	Maize *trnI/trnA* (Daniell et al., 1998)	*E. coli rrnB* 3′UTR (Tangphatsornruang et al., 2011)

(*Table continues on following page.*)

Table 1. (*Continued from previous page.*)

Promoter::5′UTR	GOI	Integration Sites	3′UTR
mP*rrn*::RBS (46%; Suzuki et al., 2003)	*Myc aadA-GFP* (Lutz et al., 2007)	Maize *trnV/3′rps12* (Staub and Maliga, 1992)	*psaC* 3′UTR (Hirose and Sugiura, 1997)
mP*rrn*::RBS (60%; Suzuki et al., 2003)	*FLARE16-S aadA-GFP* (Khan and Maliga, 1999)	Potato *trnI/trnA* (Daniell et al., 1998)	TMV 3′UTR (Kawamura-Nagaya et al., 2014)
mP*rrn*::RBS (61%; Suzuki et al., 2003)	*aac6-aph2* (Tabatabaei et al., 2017)	Potato *trnG/trnfM* (Bock and Maliga, 1995)	TYMV 3′UTR (Ma et al., 2015)
P*rrn*::RBS (Daniell et al., 2005)	*Lux-C* codon opt. tobacco chloroplasts (Lee et al., 1991)	Potato *trnV/3′ rps12* (Staub and Maliga, 1992)	BMV 3′UTR (Bujarski et al., 1985)
–	*Lux-D* codon opt. tobacco chloroplasts (Lee et al., 1991)	Potato *trnV/3′ rps12* (Staub and Maliga, 1992)	ALMV 3′UTR (Trucco et al., 2014)
–	*Lux-A* codon opt. tobacco chloroplasts (Lee et al., 1991)	–	–
–	*Lux-B* codon opt. tobacco chloroplasts (Lee et al., 1991)	–	–
–	*Lux-E* codon opt. tobacco chloroplasts (Lee et al., 1991)	–	–
–	*Lux-G* codon opt. tobacco chloroplasts (Lee et al., 1991)	–	–

comprising the *Lux* operon (*Lux-C*, *-D*, *-A*, *-B*, *-E*, and *-G*) were domesticated to Level-0 parts and assembled into Level-1 constructs (LC1, LD1, LA1, LB1, LE1, and LG1) with similar efficiency to that described previously (Table 3; Fig. 4; Supplemental Fig. S9). The seventh position in the maximum Level-2 cassette was reserved for selection using either *aadA* or *mEmerald* (Cassette S1 and S2, respectively). After sequence verification of the Level-1 constructs, Level-2 assembly of the six *Lux* cassettes, along with Cassette S1, was conducted using the potato *trnG-trnfM* Level-2 chloroplast destination vector (Fig. 5). For this test case, the assembly was designed to express seven monocistronic transcriptional units (~10.6 kb total), in which the seven genes are under the control of the same regulatory sequences (Table 3). After double selection with kanamycin/spectinomycin (*nptII* on Level-2 backbone and *aadA* within operon), it was determined that 28 of 40 colonies were PCR positive for the presence of *Lux-C*, with 26 of the 28 *Lux-C*-positive colonies positive for all genes of the operon (Supplemental Fig. S10). In this test case, the efficiency of assembly of seven Level-1 constructs into a single Level-2 construct was 65%. In the case of using *Bbs*I instead of *Bpi*I, the efficiency was substantially reduced to 1.25% (Supplemental Fig. S11). Correct assembly of the complete Level-2 operon was further validated using single-gene and junction PCR (Fig. 5). Thus, with the current design of the MoChlo kit, a single chloroplast transformation vector containing up to seven Level-1 cassettes can be assembled with high efficiency.

In Vivo Validation of the MoChlo Kit

To test functionality of the MoChlo kit and demonstrate the potential of the kit for combinatorial screening, two test operons were assembled using the methods described previously. Operon X was driven by the *rrn* promoter, and synthetic ribosome-binding site (RBS) was used as the 5′UTR. For Operon Y, the fused *accD* promoter::5′UTR were used to drive expression of the operon. In both cases, the operons were assembled into Level-2 constructs for integration into the potato *trnG-trnfM* site (Fig. 6). In both operons, *mEmerald* was used as a visual marker to verify functionality of the operon by microscopy, while a monocistronic *aadA* cassette with the fused promoter::5′UTR of *psbA* was used for antibiotic selection of transplastomic tissue. After verification of correct assembly, the Level-2 constructs were bombarded into potato leaf discs and placed under selection with spectinomycin. After ~10 weeks, primary green callus emerged indicating that the monocistronic *aadA* cassette was functional, and molecular analysis confirmed that the operons integrated correctly into the native potato plastome (Fig. 7). Further analysis of green callus by confocal microscopy showed that *mEmerald* fluorescence was present and correctly colocalized to the plastids in both operons (Fig. 6). In addition, the fluorescence intensity of

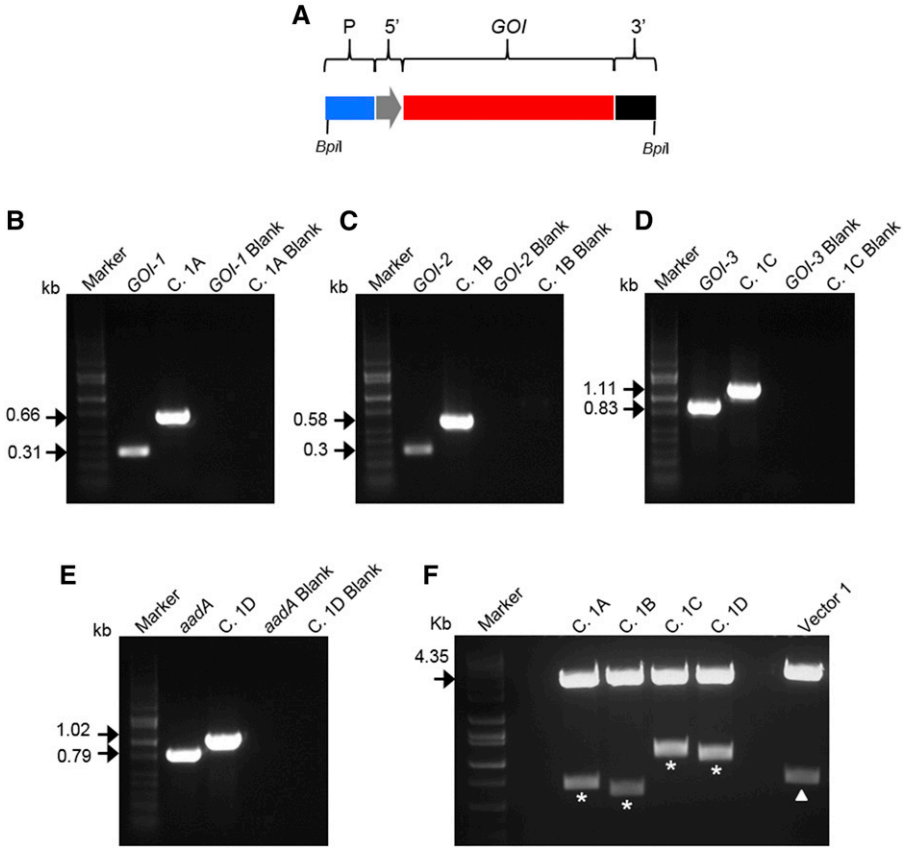

Figure 2. Level-1 cloning for a four-gene operon-1. A, Schematic representation of a Level-1 cassette: promoter (P; blue); 5′UTR (5′; gray); GOIs (*GOI1–GOI3* or *aadA*; red); terminator/3′UTR (3′; black). *Bpi*I sites flanking the Level-1 cassette are indicated. B to E, PCR to confirm Level-1 assembly. Specific primers for the internal gene (B, *GOI-1*; C, *GOI-2*; D, *GOI-3*; E, *aadA*) and the promoter/3′UTR of cassettes 1A, 1B, 1C, and 1D (B, C. 1A; C, C. 1B; D, C. 1C; E, C. 1D) have been used. DNA bands at the predicted molecular mass (kb) confirm correct Level-1 assembly of all cassettes. Negative controls (blanks) of PCR images B to E are indicated. F, *Bpi*I restriction digestion of Level-1 vectors. The four Level-1 cassettes released after digestion are indicated with asterisks (size indicated in Table 1). The empty vector 1 (vector position 1 forward) is used as a positive control. The *LacZα* fragment (0.616 kb) release after digestion of vector 1 is indicated with the triangle. The molecular mass (kb) of the backbone vector is indicated with black arrows. DNA markers are shown in each image.

mEmerald in Operon Y was weak compared with Operon X, which was expected due to the difference in regulatory elements between the operons. The ability to assemble, transform, and validate operons in ~10 weeks demonstrates the potential for the complete system for combinatorial screening of plastid regulatory elements.

DISCUSSION

In general, chloroplast biotechnology has fallen behind the current trends in synthetic biology and relies on antiquated systems for vector construction. To facilitate efficient assembly of large DNA constructs necessary for metabolic engineering, several molecular cloning methods based on Golden Gate assembly have been developed (Engler et al., 2008, 2009; Weber et al., 2011). Essentially, these methods take advantage of the unique ability of type IIS restriction enzymes to cut DNA outside of their recognition site, generating 4-bp-long nonpalindromic 5′ or 3′ overhangs (Engler et al., 2008, 2009). Cleavage sites can then be designed to produce compatible overhangs able to directionally assemble multiple DNA fragments in a one-pot, one-step reaction. By adding the same standardized overhangs to a library of DNA basic units, it is possible to generate a number of different combinations using the same cloning strategy (Sarrion-Perdigones et al., 2011; Weber et al., 2011; Lampropoulos et al., 2013). Compared with classical cloning techniques, Golden Gate assembly does not require a complicated design or time-consuming cloning. In fact, the combination of restriction digestion and ligation in a one-pot, one-step reaction eliminates the need for PCR amplification, fragment digestion, and gel purification, providing a fast and reliable method for assembly of large molecules of DNA (Weber et al., 2011). Golden Gate cloning can be performed in any laboratory equipped for molecular biology by simply purchasing enzymes (IIS

Table 2. *Design of four different Level-1 cassettes.*

Name	Promoter	5′UTR	GOI	3′UTR	Size (kb)	Position (Forward)
Cassette 1A	P*accD*	Synthetic RBS	*GOI-1*	*petD*-3′UTR	0.664	1
Cassette 1B	IEE	Synthetic RBS	*GOI-2*	*petD*-3′UTR	0.583	2
Cassette 1C	IEE	Synthetic RBS	*GOI-3*	*petD*-3′UTR	1.114	3
Cassette 1D	P*psbA*	Synthetic RBS	*aadA*	*psbA*-3′UTR	1.019	4

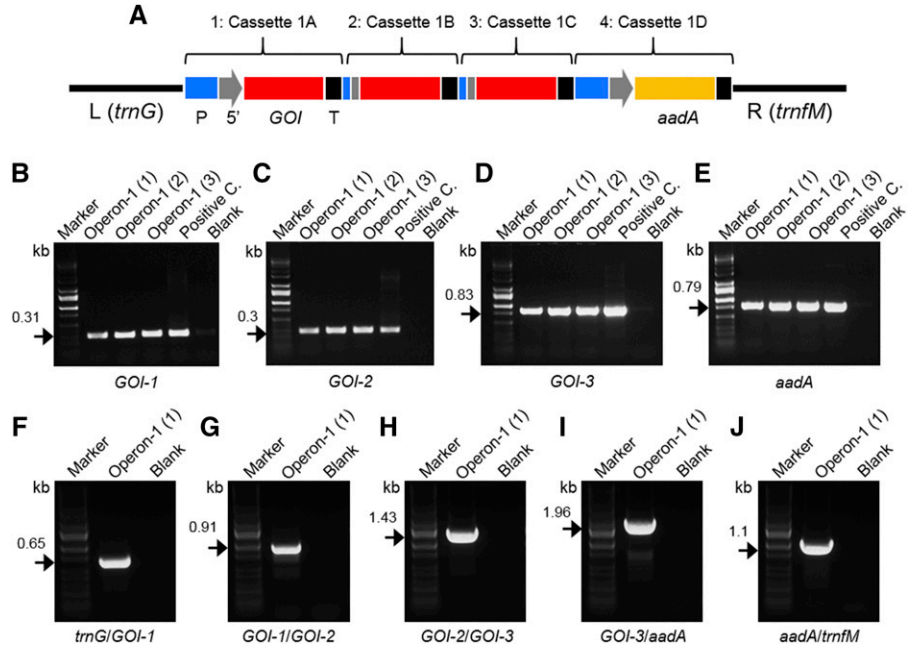

Figure 3. Level-2 cloning for operon-1. A, Schematic representation of Level-2 operon-1: promoter (P; blue); 5′UTR (5′; gray); GOIs (*GOI1*–*GOI3*; red); gene for selection (*aadA*; yellow); terminator/3′UTR (3′; black). Level-1 cassettes 1A, 1B, 1C, and 1D are assembled in positions 1, 2, 3, and 4 of operon-1, respectively. The operon-1 is cloned in a Level-2 vector between left (L; 1.17 kb) and right (R; 1.45 kb) arms homologous to the *trnG/trnfM* site of the potato plastome. B to E, PCR to confirm the presence of all genes of operon-1 (three purified vectors; 1–3). Specific primers for *GOI-1* (B), *GOI-2* (C), *GOI-3* (D), and *aadA* (E) have been used. DNA bands at the predicted molecular mass (kb; black arrows) in both purified plasmid (operon-1) and positive controls (positive C.) confirm correct Level-2 assembly of operon-1. F to J, PCR to confirm the correct order of four genes in the operon-1. Pairs or primers specific for *trnG/GOI-1* (F), *GOI-1/GOI-2* (G), *GOI-2/GOI-3* (H), *GOI-3/aadA* (I), and *aadA/trnfM* (J) have been used. DNA bands at the predicted molecular mass confirm the correct order (kb; black arrows). Negative controls (blanks) for PCR and DNA markers are shown in B to J.

restriction enzymes and T4 ligase), together with standardized DNA modules and vectors used for assembly (Marillonnet and Werner, 2015).

At present, only a single study has demonstrated the potential to utilize a modular cloning approach for the generation of chloroplast transformation vectors (Vafaee et al., 2014). In the previous work, GoldenBraid was chosen as the modular cloning strategy to demonstrate the potential for facile modular assembly of chloroplast transformation vectors. While GoldenBraid utilizes a smaller complement of destination/intermediate vectors, the number of parts that can be combined in a single step is more limited than with Golden Gate. As such, the MoChlo kit was designed using the Golden Gate MoClo approach. Considering the broad adoption of the plant MoClo kits, genes of interest developed by researchers for standard nuclear expression can be directly used in the MoChlo kit without further domestication. Furthermore, the MoChlo kit developed in this work has been released to the research community (through Addgene) with a complete set of Level-0 parts, including common chloroplast promoters, 5′UTRs, 3′UTRs, and selection genes (118 parts in total). Additionally, the kit contains Level-2 destination vectors specifically designed to enable homologous recombination into the most common sites for tobacco, maize, and potato chloroplast engineering. Also, the MoChlo kit has been validated in vivo, demonstrating the

Table 3. *Design of six Level-1 cassettes for the* Lux *operon and two Level-1 selection cassettes.*

Name	Promoter	5′UTR	GOI	3′UTR	Size (kb)	Position (Forward)
Cassette LC1	P*rrn*	P*rrn*-5′UTR	*Lux-C*	*rrnB*-3′UTR	1.919	1
Cassette LD1	P*rrn*	P*rrn*-5′UTR	*Lux-D*	*rrnB*-3′UTR	1.430	2
Cassette LA1	P*rrn*	P*rrn*-5′UTR	*Lux-A*	*rrnB*-3′UTR	1.547	3
Cassette LB1	P*rrn*	P*rrn*-5′UTR	*Lux-B*	*rrnB*-3′UTR	1.463	4
Cassette LE1	P*rrn*	P*rrn*-5′UTR	*Lux-E*	*rrnB*-3′UTR	1.604	5
Cassette LG1	P*rrn*	P*rrn*-5′UTR	*Lux-G*	*rrnB*-3′UTR	1.187	6
Cassette S1	P*rrn*	P*rrn*-5′UTR	*aadA*	*rrnB*-3′UTR	1.274	7
Cassette S2	P*rrn*	P*rrn*-5′UTR	*mEmerald*	*rrnB*-3′UTR	1.202	7

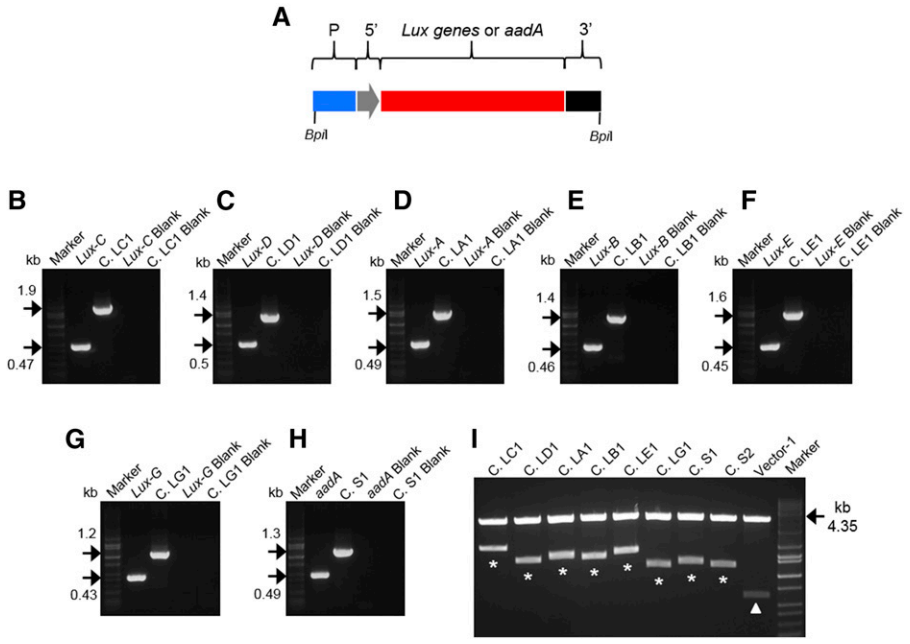

Figure 4. Level-1 cloning for the *Lux* operon for plastid engineering. A, Schematic representation of a Level-1 cassette: promoter (P; blue); 5′UTR (5′; gray); *Lux* (*C, D, A, B, E,* or *G*) or *aadA* gene for selection (red); terminator/3′UTR (3′; black). *Bpi*I sites flanking the Level-1 cassette are indicated. B to H, PCR to confirm Level-1 assembly. Specific primers for *Lux* genes (B, *Lux-C*; C, *Lux-D*; D, *Lux-A*; E, *Lux-B*; F, *Lux-E*; G, *Lux-G*), the gene for selection (H; *aadA*), and the promoter/3′UTR of cassettes LC1, LD1, LA1, LB1, LE1, LG1, and S1 (B, C. LC1; C, C. LD1; D, C. LA1; E, C. LB1; F, C. LE1; G, C. LG1; H, C. S1) have been used. DNA bands at the predicted molecular mass (kb; black arrows) confirm correct Level-1 assembly of all cassettes. Negative controls (blanks) of PCR images B to H are indicated. I, *Bpi*I restriction digestion of Level-1 vectors. Level-1 cassettes released after digestion are indicated with asterisks (cassette size indicated in Table 2). Empty vector 1 (position 1 forward) was used as a positive control. The *LacZα* fragment release after digestion of vector 1 is indicated with the arrowhead (0.616 kb). The molecular mass (kb) of the backbone vector is indicated with black arrows. DNA markers are shown in B to I.

functionality of the components and strategy. A schematic of a combinatorial study using the MoChlo kit, from assembly of constructs to the generation of transplastomic plants, is shown in Figure 8.

Of particular importance to chloroplast biotechnology is the relative dearth of information on precise control of multigene expression. Apart from developing a fast and flexible assembly method for chloroplast transformation vectors, a secondary goal of the MoChlo kit is to accelerate research into controllable multigene expression in plastids. Therefore, promoters and regulatory sequences constitute the majority of the MoChlo kit. Optimal levels of relative protein expression between different components are fundamental to achieve successful metabolic engineering. The expression levels of protein units encoded by both monocistronic DNA assemblies and synthetic operons can be manipulated both at the transcriptional and translational levels by choosing different promoters and 5′UTRs, respectively. Apart from commonly used strong promoters, such as P*rrn*, P*psbA*, and P*rbcL* (Shiina et al., 1998; Hayashi et al., 2003; Suzuki et al., 2003), the MoChlo kit has been supplemented with many other characterized and uncharacterized regulatory elements along with modified versions of endogenous promoters. As an example, point mutations within the −10 and −35 consensus sequences of *Prrn*, as well as in between them, have been shown to alter the level of transcription (Suzuki et al., 2003). Moreover, among the group of less characterized chloroplast promoters, several forms of P*atpB* (Xie and Allison, 2002), P*atpH* and P*atpI* (Miyagi et al., 1998), P*psbB* (Tanaka et al., 1987), and P*psbD* (Christopher et al., 1992; Allison and Maliga, 1995) also have been used to achieve variable gene expression. Additionally, promoters of *clpP* and *accD* have shown promise in gene expression in nongreen plastids (Zhang et al., 2012; Caroca et al., 2013). Similarly, translation motifs, such as Shine-Dalgarno sequence (or RBS) located in 5′UTRs, are important for efficient translation of protein. In the MoChlo kit, we provide a library of endogenous 5′UTRs and modified versions that are characterized by different translation efficiencies. Therefore, by using both modified versions of the same 5′UTR and sequences from different genes, it is possible to manipulate protein translation. For example, deletion of either *psbA* RBS1 or RBS2 reduces translation efficiency by ~30%, whereas the disruption of both sequences has a drastic effect on protein translation. In contrast, deletion of the third RBS of the *psbA* 5′UTR has little effect on protein translation (Hirose and Sugiura, 1996). Similarly, mutation of the Shine-Dalgarno sequence of the *rps2* 5′UTR resulted in

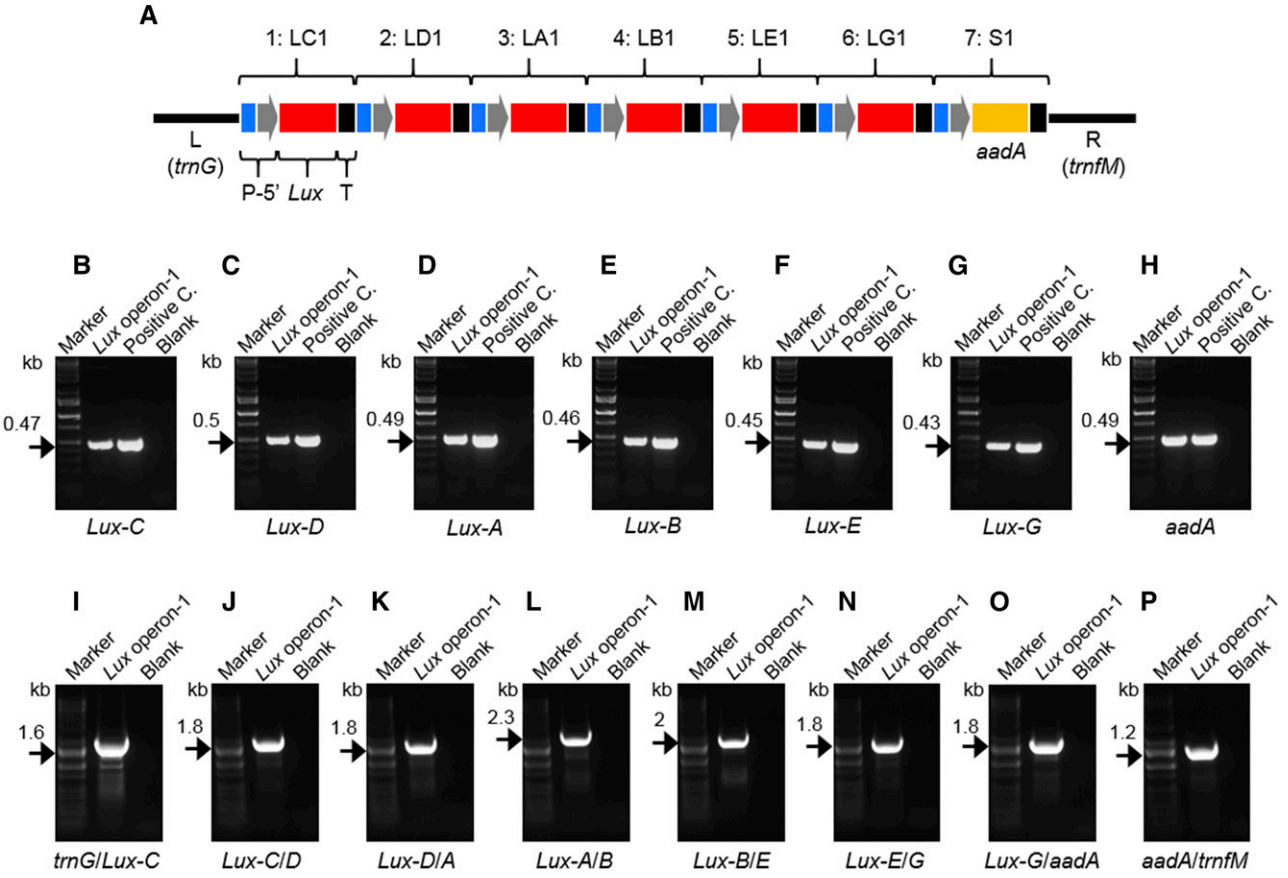

Figure 5. Level-2 cloning for the seven-gene *Lux* operon. A, Schematic representation of Level-2 assembly of *Lux* operon-1: promoter (P; blue); 5′UTR (5′; gray); *Lux* (*C*, *D*, *A*, *B*, *E*, or *G*; red); gene for selection (*aadA*; yellow); terminator/3′UTR (3′; black). Level-1 cassettes LC1, LD1, LA1, LB1, LE1, LG1, and S1 are assembled in operon positions 1, 2, 3, 4, 5, 6, and 7, respectively. The *Lux* operon-1 is cloned in Level-2 vector between left (L; 1.17 kb) and right (R; 1.45 kb) arms homologous to the *trnG/trnfM* site of the potato plastome. B to H, PCR of all genes of the *Lux* operon-1. Primers specific for *Lux-C* (B), *Lux-D* (C), *Lux-A* (D), *Lux-B* (E), *Lux-E* (F), *Lux-G* (G), and *aadA* (H) have been used. DNA bands at the predicted molecular mass (kb; black arrows) for both purified plasmid (*Lux* operon-1) and positive controls (positive C.) confirmed the presence of all genes. I to P, PCR to check correct gene order in the *Lux* operon-1. Pairs or primers specific for *trnG/Lux-C* (I), *Lux-C/Lux-D* (J), *Lux-D/Lux-A* (K), *Lux-A/Lux-B* (L), *Lux-B/Lux-E* (M), *Lux-E/Lux-G* (N), *Lux-G/aadA* (O), and *aadA/trnfM* (P) have been used. DNA bands (black arrows) at the predicted molecular mass (kb) confirm correct gene order. Negative controls (blanks) of PCR and DNA markers are shown in B to P.

severalfold increase in translation efficiency compared with the wild-type sequence (Plader and Sugiura, 2003). Processed forms of 5′UTRs of *psbN* and *psbB* have also been shown to significantly affect translation efficiency (Yukawa et al., 2007; Kuroda and Sugiura, 2014). A chimeric synthetic 5′UTR generated from *psbA-rbcL* has also been demonstrated with a 1.5-fold decrease of translation efficiency compared with the wild-type sequences (Zou et al., 2003). Considering that the goal of many of these earlier works was to maximize transcription and translation of transgenes, many characterized regulatory elements have fallen by the wayside.

A key component for broad adoption of the MoChlo kit, and thus its usefulness to the research community, is its ease of use and efficiency. In our hands, the MoChlo kit provides a robust assembly strategy for chloroplast transformation vectors containing up to seven different cassettes. A fundamental point of emphasis for achieving high-efficiency assembly was the choice of the IIS restriction enzyme. For assembly of chloroplast transformation vectors containing only two cassettes, the choice in enzyme between *Bbs*I and *Bpi*I was irrelevant (Supplemental Fig. S7). For Level-2 assembly of three or more cassettes, a much higher efficiency of assembly was achieved by using *Bpi*I rather than the isoschizomer *Bbs*I. Attempts to assemble four- and seven-gene operons using *Bbs*I resulted in efficiencies of 22.5% and 1.25% (Supplemental Figs. S5 and S11), compared with 92.5% and 65% using *Bpi*I (Supplemental Figs. S6 and S10). One possible reason for the decrease in efficiency of assembly could be the kinetic properties of the two enzymes. The one-pot, one-step reaction is performed in T4 DNA ligase buffer, and we postulate that *Bpi*I has more favorable kinetics in this suboptimal buffer.

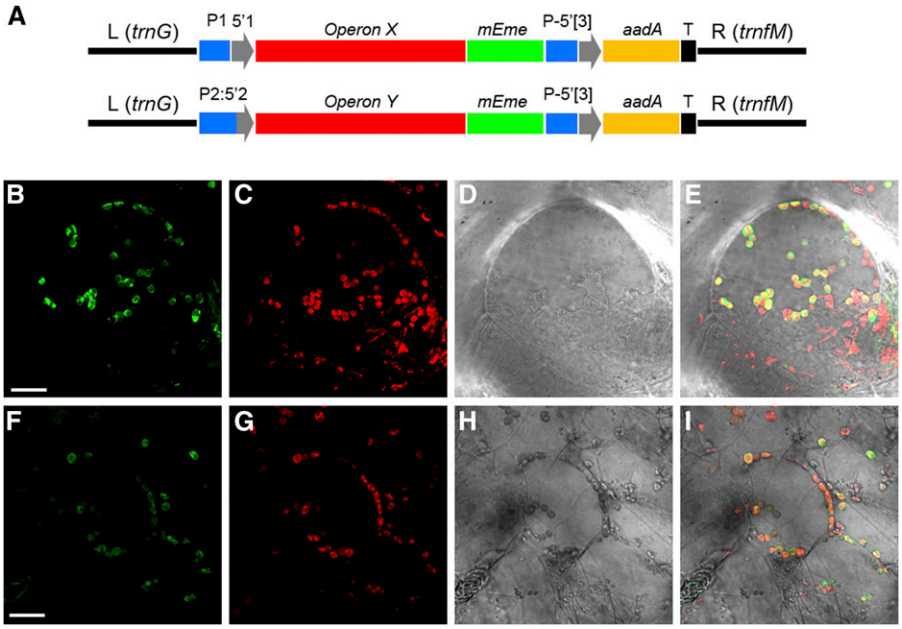

Figure 6. An example of in vivo validation of two MoChlo-enabled constructs in potato chloroplasts. A, Schematic representation of test operons controlled by two examples of promoter::5′UTR combinations. The operon (red) is controlled by the *rrn* promoter (P1) along with a synthetic RBS as 5′UTR (5′1; blue and gray; Operon X) or the promoter::5′UTR fusion of *accD* gene (P2:5′2; blue and gray; Operon Y). The expression of *mEmerald* (*mEme*; green) is under the control of the operon promoter, while the selection gene, *aadA* (yellow), is under the control of both promoter::5′UTR (P-5′[3]; blue and gray) and terminator/3′UTR (T; black) of the *psbA* gene. B to I, Confocal images of transplastomic green callus transformed with Operon X (B–E) or Operon Y (F–I). In both cases, the mEmerald fluorescent signal is localized to chloroplasts. B and F show mEmerald signal; C and G show chlorophyll autofluorescence; D and H show bright-field images; and E and I show merged images. Bars = 20 μm for all confocal images.

Moreover, *Bbs*I has lower thermal stability that may reduce its activity during the Golden Gate reaction. In any event, the MoChlo kit provides a considerable advantage to small labs with limited resources and funding, in that only the genes of interest must be synthesized, and complete assembly can be accomplished using only two enzymes.

In its current form, the MoChlo kit was designed to allow assembly of seven transcriptional units into a single chloroplast transformation vector. Considering the high efficiency obtained for the maximum test case, it would be useful to identify the upper limit for efficient assembly of a chloroplast transformation vector. In a previous study, 11 Level-1 cassettes consisting of 44 Level-0 modules were assembled into a 33-kb DNA fragment using Golden Gate assembly (Weber et al., 2011). In future iterations of the MoChlo kit, the system will be expanded to assemble larger and more complex synthetic operons. For this purpose, a new set of Level-2 end linkers equipped with a visual marker (e.g. *LacZα*) flanked by different IIS restriction sites (*Bsa*I or *Eps*3I) will be synthesized. The generation of compatible overhangs after restriction digestion will allow an additional Level-3 directional cloning to insert more transcriptional units into preassembled Level-2 constructs. Considering the relatively small size of the complete chloroplast genome of land plants (~100–200 kb), it would theoretically be possible to synthesize a complete synthetic chloroplast genome using this approach.

CONCLUSION

The main goal of the MoChlo kit developed in this work was to provide a standardized method to assemble multigene constructs for metabolic engineering using presynthesized chloroplast destination vectors and a wide array of regulatory elements. The library of Level-0 parts developed in this work provides both commonly used and uncharacterized plastid regulatory sequences, allowing for precise modulation of multiple genes necessary to guarantee optimal protein stoichiometry for metabolic engineering. With the modularity of the approach, the MoChlo kit can be expanded easily by adding new regulatory sequences (e.g. prokaryotic inducible promoters), protein tags (e.g. fluorescent proteins and epitopes), and species-specific integration sites, along with a set of new linkers that could extend the number of transcriptional units (greater than seven) currently allowable in the kit. The substantial decrease in the cost of gene synthesis further facilitates use of the kit by researchers with limited funding and resources. The creation of a common resource of standardized Level-0 parts will provide enormous advantages in terms of collaboration and accessibility to researchers

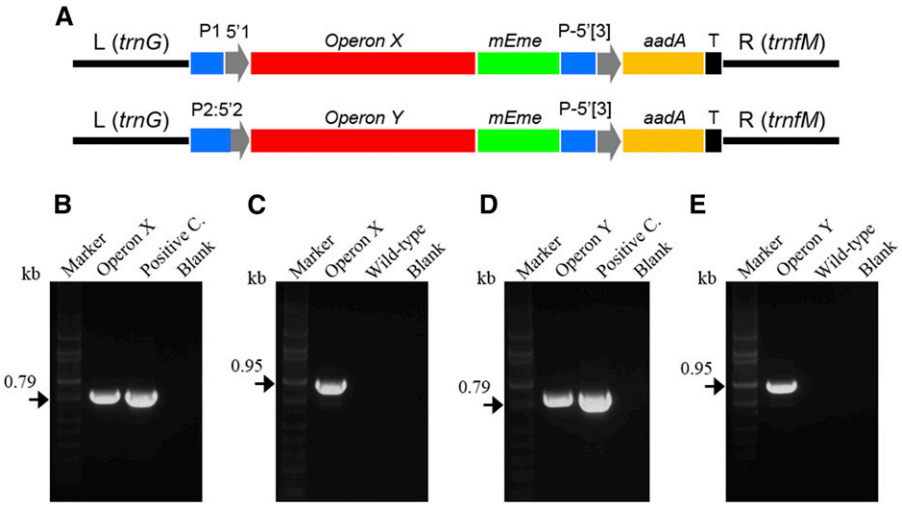

Figure 7. Operon integration in the potato plastome. A, Schematic representation of chloroplast constructs: *rrn* promoter (P1) along with a synthetic RBS used as 5′UTR (5′1; blue and gray); promoter::5′UTR fusion of *accD* gene (P2:5′2; blue and gray); P-5′[3], promoter::5′UTR of the *psbA* gene (blue and gray); T, terminator/3′UTR of *psbA* gene (black); *operon X* and *Y* (red); *mEme* (mEmerald fluorescent marker; green); and *aadA* (3′-adenylyltransferase selection marker; yellow). The left (L; 1.17 kb) and right (R; 1.45 kb) arms homologous to the *trnG/trnfM* site of the potato plastome are indicated. B to E, PCR on total genomic DNA extracted from transplastomic green callus transformed with *Operon X* (B and C) or *Operon Y* (D and E). A pair of primers specific for the *aadA* gene (B and D) and *aadA/trnfM* (C and E) have been used to check correct operon integration. DNA bands at the predicted molecular mass confirm correct integration of both operons (kb; black arrows in B–E and black line in A). Positive and negative controls (blanks) along with potato wild-type samples and DNA markers are shown.

working in chloroplast biotechnology. Furthermore, the MoChlo assembly strategy is highly amenable to automation, which may further drive the potential for combinatorial screening of numerous metabolic engineering cassettes for plastid engineering.

MATERIALS AND METHODS

Design of Modules for Golden Gate Assembly

To generate Level-0 parts, the nucleotide sequences of chloroplast regulatory elements (promoters, 5′UTRs, and 3′UTRs) and genes (fluorescent/selective markers, *Lux* genes, and *GOIs*) were domesticated with both 5′ and 3′ overhangs using the criteria set forth previously (Supplemental Fig. S1; Weber et al., 2011; Engler et al., 2014). First, all IIS restriction sites (*Bsa*I, *Bpi*I, and *Esp*3I) in the native part sequences were removed by single nucleotide substitutions. Next, the parts were flanked by *Bsa*I sites at opposite orientation along with synthetic cut sites that generate 5′ and 3′ overhangs after restriction digestion. The resulting overhangs guarantee specific directional cloning of Level-0 parts into Level-1 transcriptional units following the order promoter-5′UTR-GOI-3′UTR (Fig. 1; Supplemental Fig. S1). Compatible overhangs for Level-1 assembly and possible combinations of Level-0 parts are shown in Supplemental Figure S1. Level-0 modules of the same functional group are equipped with identical overhangs, allowing the generation of different cassettes by choosing specific modules of interest. The 5′ overhang of Level-0 promoters and the 3′ overhang of 3′UTRs were designed to ligate to compatible ends of Level-1 destination vectors. The overhangs used in the MoChlo kit were specifically designed to be compatible with vectors generated in previous plant MoClo systems (Engler et al., 2014). Finally, Level-0 and homologous sequences of chloroplast destination vectors were chemically synthesized by GeneArt (Invitrogen, Thermo Fisher Scientific) and cloned into *Escherichia coli* pUC-based vectors (kanamycin resistance gene *nptII*). The codon usage of *Lux* genes and *GOI-1*, *GOI-2*, and *GOI-3* were optimized for the tobacco (*Nicotiana tabacum*) chloroplast genome using Optimizer (Evolutionary Genomics Group, Biochemistry and Biotechnology Department, Universitat Rovira i Virgili, Tarragona, Spain; http://genomes.urv.es/OPTIMIZER/) and a codon usage table downloaded from the codon usage database (http://www.kazusa.or.jp/codon/). Level-1 destination vectors and Level-2 end linkers from previous studies were used directly (Weber et al., 2011; Engler et al., 2014).

Golden Gate Cloning and Transformation in *Escherichia coli*

The one-pot, one-step reaction for Golden Gate cloning was performed in a total volume of 20 μL adding the following components in the same PCR tube. (1) Twenty-five nanograms of destination vector either for Level-1 or Level-2 and a variable amount of individual plasmids containing the fragments of interest. One hundred nanograms of plasmid containing the larger fragment along with variable amounts (ng) of other plasmids with different M_r levels. The amount of all plasmids was adjusted to guarantee the same molar ratio for all components. For Level-2, 50 ng of plasmid containing the correct end linker was also added. (2) One microliter (20 units) of the correct IIS restriction enzyme. *Bsa*I (*Bsa*I HF V2; New England Biolabs) was used for Level-1 and either *Bpi*I (Anza 4 *Bpi*I; Invitrogen, Thermo Fisher Scientific) or *Bbs*I (*Bbs*I HF; New England Biolabs) was used for Level-2. *Bpi*I was used for operons larger than two cassettes. (3) One microliter (400 units) of T4 DNA ligase (New England Biolabs). (4) Two microliters of T4 DNA ligase buffer (10× stock), and the final volume was adjusted to 20 μL using sterile ultrapure water.

The Golden Gate reactions for both Level-1 and Level-2 were performed overnight in a thermocycler. A first step of 10 min at 37°C and then 10 min at 16°C was repeated for 35 cycles. The reaction was then incubated at 50°C for 30 min and 60 more min at 16°C. Before transformation into *E. coli*, the enzymes were inactivated for 20 min at 65°C. One microliter of Golden Gate reaction was added to 25 μL of TOP10 Chemically Competent *E. coli* (Invitrogen, Thermo Fisher Scientific) and transformed by the heat shock method (according to the manufacturer's protocol). After transformation, 250 μL of super optimal broth medium (Invitrogen, Thermo Fisher Scientific) was added and then incubated for 1 h at 37°C under agitation. Fifty microliters of bacteria cultures was plated on a petri dish containing LB-agar (Luria-Bertani medium: 10 g L^{-1} tryptone, 10 g L^{-1} NaCl, 5 g L^{-1} yeast extract, and 15 g L^{-1} bacto-agar, pH 7) containing the correct selective agent. Kanamycin and spectinomycin were used at 50 and 100 μg mL^{-1}, respectively. Liquid bacterial cultures were grown in Luria-Bertani medium without bacto-agar.

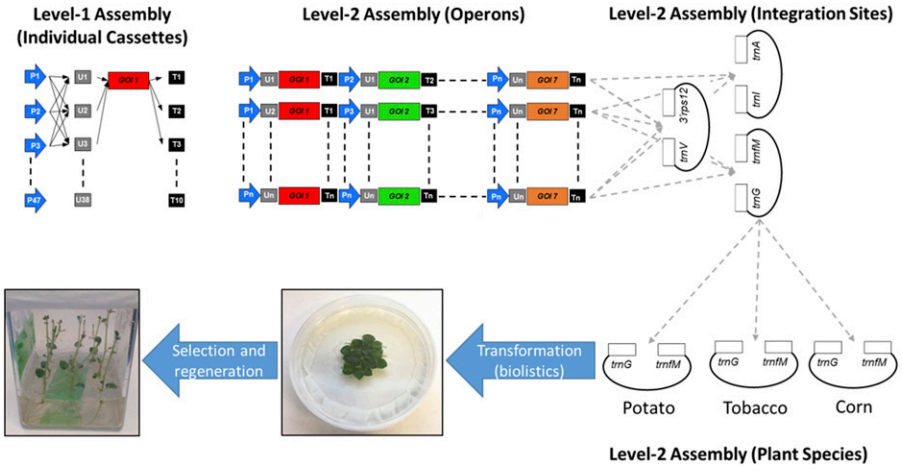

Figure 8. Schematic of the MoChlo kit for combinatorial assembly of operons for metabolic engineering. In the current iteration of the kit, combinatorial assembly of individual cassettes (Level-1 constructs) can be conducted using 47 promoters, 38 5′UTRs, nine promoter:5′UTR fusions, and 10 terminators/3′UTRs. In addition, the user has the ability to assemble up to seven individual cassettes, each with its own regulatory elements and GOIs. Furthermore, during Level-2 assembly, the user can choose from three different integration sites (*trnI-trnA*, *trnV-3′rps12*, and *trnG-trnfM*) from three different plant species (tobacco, maize, and potato). After completing assembly, the user would then bombard the Level-2 constructs into leaf discs and select and regenerate transplastomic plants.

Plasmid Extraction from Bacterial Cells, Restriction Digestion, and PCR

Pure plasmid preparations were obtained using QIAprep Spin Miniprep Kit (Qiagen). The restriction digestions using either *Bsa*I or *Bbs*I (New England Biolabs) were performed in a total volume of 30 μL using 10 units of enzyme, 500 ng of plasmid, and 1× Custom buffer (New England Biolabs). The restriction digestion using *Bpi*I was performed using the same conditions in Anza 1× buffer (Invitrogen, Thermo Fisher Scientific). PCRs were performed in 25-μL reaction volumes using 1× DreamTaq Green PCR Master Mix (Thermo Fisher Scientific), along with specific pairs of primers and 25 ng of template plasmid. For colony PCR, the reactions were performed using 2 μL of overnight bacteria liquid cultures. The following combinations of forward/reverse primers were used to amplify the indicated DNA fragments: *GOI-1*, primers 1/20; *GOI-2*, primers 2/21; *GOI-3*, primers 3/22; *GOI-4*, primers 4/23; *aadA* (full length), primers 5/24; Cassette 1A, primers 6/25; Cassette 1B and 1C, primers 7/25; Cassette 1D, primers 8/26; *trnG/GOI-1*, primers 9/20; *GOI-1/GOI-2*, primers 1/21; *GOI-2/GOI-3*, primers 2/22; *GOI-3/aadA*, primers 3/24; *aadA/trnfM*, primers 5/27; *Lux-C*, primers 10/28; *Lux-D*, primers 11/29; *Lux-A*, primers 12/30; *Lux-B*, primers 13/31; *Lux-E*, primers 14/32; *Lux-G*, primers 15/33; *aadA* (fragment), primers 16/34; *mEmerald* (fragment), primers 17/35; Cassette LC1, LD1, LA1, LB1, LE1, LG1, and S1, primers 18/36; *trnG/Lux-C*, primers 9/28; *Lux-C/Lux-D*, primers 10/29; *Lux-D/Lux-A*, primers 11/30; *Lux-A/Lux-B*, primers 12/31; *Lux-B/Lux-E*, primers 13/32; *Lux-E/Lux-G*, primers 14/33; *Lux-G/aadA*, primers 15/34; *aadA/trnfM*, primers 5/27; and right and left of T-DNA, primers 19/37. A list of primers used in this work is shown in Supplemental Table S4. Both restriction digestion and PCR products were separated by electrophoresis using 1% (w/v) agarose gel in 1× TAE buffer (40 mM Tris-acetate and 1 mM EDTA, pH 8.3) containing 0.3 μg mL^{-1} ethidium bromide. The Hi-Lo DNA ladder from 50 to 10,000 bp (BIONEXUS) was used as a molecular DNA marker.

Transformation, Selection, and Screening of Potato Chloroplasts

Potato (*Solanum tuberosum* var 'Desirée') was grown in sterile conditions in Magenta boxes containing MS Reg. medium (4.33 g L^{-1} Murashige and Skoog basal salt mixture, 25 g L^{-1} Suc, 100 mg L^{-1} myoinositol, 170 mg L^{-1} sodium phosphate monobasic monohydrate, 440 mg L^{-1} calcium chloride dihydrate, 0.9 mg L^{-1} thiamine-HCl, 2 mg L^{-1} Gly, 0.5 mg L^{-1} nicotinic acid, 0.5 mg L^{-1} pyridoxine-HCl, 1× Murashige and Skoog vitamins, and 3 g L^{-1} phytagel, pH 5.8). Potato plants were kept in a controlled growth room with 16 h of light (100 μmol m^{-2} s^{-1}) and 8 h of dark. The temperature was kept at 24°C constant during all light/dark cycles. Transplastomic green callus was obtained from biolistic transformation of potato leaf discs as described previously (Valkov et al., 2014). Briefly, DNA constructs were bound on the surface of 600-nm gold particles (Seashell Technology) and bombarded into potato leaf discs on M6M medium. Selection of transplastomic green callus was obtained by subculturing leaf discs in M6 medium (~4 weeks) and Ti medium (~6 weeks) with spectinomycin, as described previously (Valkov et al., 2014).

To confirm integration, a cetyl-trimethyl-ammonium bromide-based procedure was used to extract total genomic DNA from green callus prior to confirmation of integration of the transplastomic cassette by PCR (Lin et al., 2014b). After isolation, 5 to 10 ng of total genomic DNA was used as template for PCR as described previously. The primers 5/24 and 16/27 were used to detect the full-length *aadA* gene and the *aadA/trnfM* integration region, respectively (Supplemental Table S4). Transplastomic green callus was imaged using an Olympus Fv1000 confocal microscope. The mEmerald fluorescent protein was excited at 488 nm and detected at 505 to 530 nm. Chlorophyll autofluorescence was obtained using excitation at 543 nm and detection at greater than 560 nm. Digital images were acquired using the Olympus FV10-ASW Viewer software Ver.4.2a. Confocal images were processed using ImageJ 1.41o (National Institutes of Health).

Accession Numbers

Sequences of native regulatory elements and homology arms were mined from the native plastid genomes of tobacco (Z00044.2), potato (DQ231562.1), and maize (NC_001666.2), while the *E. coli* terminator for *rrnB* (CP034595.1) and viral terminators from *Tobacco mosaic virus* (MK087763.1), *Turnip yellow mosaic virus* (KP995420.1), *Brome mosaic virus* (M12024.1), and *Alfalfa mosaic virus* (KC881009.1) were mined from their respective genomes. In addition, marker and selection genes for *mEmerald* (BAU94259.1), *pporRFP* (ABB17953.1), *aadA* (ARK38551.1), *aphA6* (AZR92252.1), *nptII* (ASU89325.1), *myc-aadA-GFP* (AAF65230.1), *FLARE16-S aadA-GFP* (AAF65229.1), *aac6-aph2* (WP_001028144.1), and the complete *Lux* operon from *Photobacterium leiognathi* (M63594.1) were mined from GenBank. All sequences were domesticated for use in the MoChlo kit as previously described, and the sequences of all Level-0 modules are included in Supplemental Table S1, with the entire MoChlo kit available from Addgene.

Supplemental Data

The following supplemental materials are available.

Supplemental Figure S1. Level-0 modules and directional cloning into Level-1 cassettes.

Supplemental Figure S2. Directional cloning of Level-1 cassettes into operons of different lengths.

Supplemental Figure S3. Level-1 assembly of GOIs.

Supplemental Figure S4. Examples of Level-1 cassettes synthesized using the MoChlo kit.

Supplemental Figure S5. Colony screening for Level-2 assembly of operon-1 using *Bbs*I in the Golden Gate reaction.

Supplemental Figure S6. Colony screening for Level-2 assembly of operon-1 using *Bpi*I in the Golden Gate reaction.

Supplemental Figure S7. Level-2 assembly of two-gene selection cassettes using *Bbs*I in the Golden Gate reaction.

Supplemental Figure S8. Level-2 assembly of five different four-gene operons.

Supplemental Figure S9. Level-1 assembly of Level-1 *Lux* cassettes.

Supplemental Figure S10. Colony screening for Level-2 assembly of *Lux* operon-1 using *Bpi*I in the Golden Gate reaction.

Supplemental Figure S11. Colony screening for Level-2 assembly of *Lux* operon-1 using *Bbs*I in the Golden Gate reaction.

Supplemental Table S1. MoChlo Level-0 modules.

Supplemental Table S2. Level-1 vectors compatible for the MoChlo kit.

Supplemental Table S3. Level-2 end linkers and Level-2 chloroplast destination vectors.

Supplemental Table S4. Primers used in this study.

ACKNOWLEDGMENTS

We thank Holly Baxter and Sidney Vafaie-Partin for providing technical support throughout the project.

Received October 3, 2018; accepted January 16, 2019; published January 24, 2019.

LITERATURE CITED

Alieva NO, Konzen KA, Field SF, Meleshkevitch EA, Hunt ME, Beltran-Ramirez V, Miller DJ, Wiedenmann J, Salih A, Matz MV (2008) Diversity and evolution of coral fluorescent proteins. PLoS ONE **3:** e2680

Allison LA, Maliga P (1995) Light-responsive and transcription-enhancing elements regulate the plastid psbD core promoter. EMBO J **14:** 3721–3730

Allison LA, Simon LD, Maliga P (1996) Deletion of rpoB reveals a second distinct transcription system in plastids of higher plants. EMBO J **15:** 2802–2809

Apel W, Bock R (2009) Enhancement of carotenoid biosynthesis in transplastomic tomatoes by induced lycopene-to-provitamin A conversion. Plant Physiol **151:** 59–66

Baecker JJ, Sneddon JC, Hollingsworth MJ (2009) Efficient translation in chloroplasts requires element(s) upstream of the putative ribosome binding site from atpI. Am J Bot **96:** 627–636

Bock R (2013) Strategies for metabolic pathway engineering with multiple transgenes. Plant Mol Biol **83:** 21–31

Bock R (2015) Engineering plastid genomes: Methods, tools, and applications in basic research and biotechnology. Annu Rev Plant Biol **66:** 211–241

Bock R, Maliga P (1995) *In vivo* testing of a tobacco plastid DNA segment for guide RNA function in psbL editing. Mol Gen Genet **247:** 439–443

Boyhan D, Daniell H (2011) Low-cost production of proinsulin in tobacco and lettuce chloroplasts for injectable or oral delivery of functional insulin and C-peptide. Plant Biotechnol J **9:** 585–598

Bujarski JJ, Dreher TW, Hall TC (1985) Deletions in the 3′-terminal tRNA-like structure of brome mosaic virus RNA differentially affect aminoacylation and replication in vitro. Proc Natl Acad Sci USA **82:** 5636–5640

Caroca R, Howell KA, Hasse C, Ruf S, Bock R (2013) Design of chimeric expression elements that confer high-level gene activity in chromoplasts. Plant J **73:** 368–379

Carrer H, Hockenberry TN, Svab Z, Maliga P (1993) Kanamycin resistance as a selectable marker for plastid transformation in tobacco. Mol Gen Genet **241:** 49–56

Christopher DA, Kim M, Mullet JE (1992) A novel light-regulated promoter is conserved in cereal and dicot chloroplasts. Plant Cell **4:** 785–798

Cubitt AB, Woollenweber LA, Heim R (1999) Understanding structure-function relationships in the *Aequorea victoria* green fluorescent protein. Methods Cell Biol **58:** 19–30

Daniell H, Datta R, Varma S, Gray S, Lee SB (1998) Containment of herbicide resistance through genetic engineering of the chloroplast genome. Nat Biotechnol **16:** 345–348

Daniell H, Chebolu S, Kumar S, Singleton M, Falconer R (2005) Chloroplast-derived vaccine antigens and other therapeutic proteins. Vaccine **23:** 1779–1783

Davoodi-Semiromi A, Schreiber M, Nalapalli S, Verma D, Singh ND, Banks RK, Chakrabarti D, Daniell H (2010) Chloroplast-derived vaccine antigens confer dual immunity against cholera and malaria by oral or injectable delivery. Plant Biotechnol J **8:** 223–242

Eibl C, Zou Z, Beck A, Kim M, Mullet J, Koop HU (1999) *In vivo* analysis of plastid psbA, rbcL and rpl32 UTR elements by chloroplast transformation: Tobacco plastid gene expression is controlled by modulation of transcript levels and translation efficiency. Plant J **19:** 333–345

Emadpour M, Karcher D, Bock R (2015) Boosting riboswitch efficiency by RNA amplification. Nucleic Acids Res **43:** e66

Engler C, Kandzia R, Marillonnet S (2008) A one pot, one step, precision cloning method with high throughput capability. PLoS ONE **3:** e3647

Engler C, Gruetzner R, Kandzia R, Marillonnet S (2009) Golden gate shuffling: A one-pot DNA shuffling method based on type IIs restriction enzymes. PLoS ONE **4:** e5553

Engler C, Youles M, Gruetzner R, Ehnert TM, Werner S, Jones JD, Patron NJ, Marillonnet S (2014) A golden gate modular cloning toolbox for plants. ACS Synth Biol **3:** 839–843

Fuentes P, Zhou F, Erban A, Karcher D, Kopka J, Bock R (2016) A new synthetic biology approach allows transfer of an entire metabolic pathway from a medicinal plant to a biomass crop. eLife **5:** e13664

Hammani K, Cook WB, Barkan A (2012) RNA binding and RNA remodeling activities of the half-a-tetratricopeptide (HAT) protein HCF107 underlie its effects on gene expression. Proc Natl Acad Sci USA **109:** 5651–5656

Hayashi K, Shiina T, Ishii N, Iwai K, Ishizaki Y, Morikawa K, Toyoshima Y (2003) A role of the −35 element in the initiation of transcription at psbA promoter in tobacco plastids. Plant Cell Physiol **44:** 334–341

Hirata N, Yonekura D, Yanagisawa S, Iba K (2004) Possible involvement of the 5′-flanking region and the 5′UTR of plastid accD gene in NEP-dependent transcription. Plant Cell Physiol **45:** 176–186

Hirose T, Sugiura M (1996) Cis-acting elements and trans-acting factors for accurate translation of chloroplast psbA mRNAs: Development of an *in vitro* translation system from tobacco chloroplasts. EMBO J **15:** 1687–1695

Hirose T, Sugiura M (1997) Both RNA editing and RNA cleavage are required for translation of tobacco chloroplast ndhD mRNA: A possible regulatory mechanism for the expression of a chloroplast operon consisting of functionally unrelated genes. EMBO J **16:** 6804–6811

Hirose T, Sugiura M (2004) Multiple elements required for translation of plastid atpB mRNA lacking the Shine-Dalgarno sequence. Nucleic Acids Res **32:** 3503–3510

Hirose T, Kusumegi T, Sugiura M (1998) Translation of tobacco chloroplast rps14 mRNA depends on a Shine-Dalgarno-like sequence in the 5′-untranslated region but not on internal RNA editing in the coding region. FEBS Lett **430:** 257–260

Huang FC, Klaus SM, Herz S, Zou Z, Koop HU, Golds TJ (2002) Efficient plastid transformation in tobacco using the aphA-6 gene and kanamycin selection. Mol Genet Genomics **268:** 19–27

Jin S, Daniell H (2015) The engineered chloroplast genome just got smarter. Trends Plant Sci **20:** 622–640

Kawamura-Nagaya K, Ishibashi K, Huang YP, Miyashita S, Ishikawa M (2014) Replication protein of tobacco mosaic virus cotranslationally

binds the 5′ untranslated region of genomic RNA to enable viral replication. Proc Natl Acad Sci USA **111:** E1620–E1628

Khan MS, Maliga P (1999) Fluorescent antibiotic resistance marker for tracking plastid transformation in higher plants. Nat Biotechnol **17:** 910–915

Kuroda H, Maliga P (2001a) Complementarity of the 16S rRNA penultimate stem with sequences downstream of the AUG destabilizes the plastid mRNAs. Nucleic Acids Res **29:** 970–975

Kuroda H, Maliga P (2001b) Sequences downstream of the translation initiation codon are important determinants of translation efficiency in chloroplasts. Plant Physiol **125:** 430–436

Kuroda H, Maliga P (2002) Overexpression of the clpP 5′-untranslated region in a chimeric context causes a mutant phenotype, suggesting competition for a clpP-specific RNA maturation factor in tobacco chloroplasts. Plant Physiol **129:** 1600–1606

Kuroda H, Sugiura M (2014) Processing of the 5′-UTR and existence of protein factors that regulate translation of tobacco chloroplast psbN mRNA. Plant Mol Biol **86:** 585–593

Kuroda H, Suzuki H, Kusumegi T, Hirose T, Yukawa Y, Sugiura M (2007) Translation of psbC mRNAs starts from the downstream GUG, not the upstream AUG, and requires the extended Shine-Dalgarno sequence in tobacco chloroplasts. Plant Cell Physiol **48:** 1374–1378

Lakshmi PS, Verma D, Yang X, Lloyd B, Daniell H (2013) Low cost tuberculosis vaccine antigens in capsules: Expression in chloroplasts, bioencapsulation, stability and functional evaluation *in vitro*. PLoS ONE **8:** e54708

Lampropoulos A, Sutikovic Z, Wenzl C, Maegele I, Lohmann JU, Forner J (2013) GreenGate: A novel, versatile, and efficient cloning system for plant transgenesis. PLoS ONE **8:** e83043

Lee CY, Szittner RB, Meighen EA (1991) The lux genes of the luminous bacterial symbiont, *Photobacterium leiognathi*, of the ponyfish: Nucleotide sequence, difference in gene organization, and high expression in mutant *Escherichia coli*. Eur J Biochem **201:** 161–167

Liere K, Maliga P (1999) *In vitro* characterization of the tobacco rpoB promoter reveals a core sequence motif conserved between phage-type plastid and plant mitochondrial promoters. EMBO J **18:** 249–257

Lin MT, Occhialini A, Andralojc PJ, Devonshire J, Hines KM, Parry MA, Hanson MR (2014a) β-Carboxysomal proteins assemble into highly organized structures in Nicotiana chloroplasts. Plant J **79:** 1–12

Lin MT, Occhialini A, Andralojc PJ, Parry MA, Hanson MR (2014b) A faster Rubisco with potential to increase photosynthesis in crops. Nature **513:** 547–550

Long BM, Hee WY, Sharwood RE, Rae BD, Kaines S, Lim YL, Nguyen ND, Massey B, Bala S, von Caemmerer S, et al (2018) Carboxysome encapsulation of the CO_2-fixing enzyme Rubisco in tobacco chloroplasts. Nat Commun **9:** 3570

Lu Y, Rijzaani H, Karcher D, Ruf S, Bock R (2013) Efficient metabolic pathway engineering in transgenic tobacco and tomato plastids with synthetic multigene operons. Proc Natl Acad Sci USA **110:** E623–E632

Lutz KA, Azhagiri AK, Tungsuchat-Huang T, Maliga P (2007) A guide to choosing vectors for transformation of the plastid genome of higher plants. Plant Physiol **145:** 1201–1210

Ma J, Pallett D, Jiang H, Hou Y, Wang H (2015) Mutational bias of Turnip Yellow Mosaic Virus in the context of host anti-viral gene silencing. Virology **486:** 2–6

Maliga P (2004) Plastid transformation in higher plants. Annu Rev Plant Biol **55:** 289–313

Maliga P, Bock R (2011) Plastid biotechnology: Food, fuel, and medicine for the 21st century. Plant Physiol **155:** 1501–1510

Marillonnet S, Werner S (2015) Assembly of multigene constructs using Golden Gate cloning. Methods Mol Biol **1321:** 269–284

McNeal JR, Kuehl JV, Boore JL, de Pamphilis CW (2007) Complete plastid genome sequences suggest strong selection for retention of photosynthetic genes in the parasitic plant genus *Cuscuta*. BMC Plant Biol **7:** 57

Miyagi T, Kapoor S, Sugita M, Sugiura M (1998) Transcript analysis of the tobacco plastid operon rps2/atpI/H/F/A reveals the existence of a nonconsensus type II (NCII) promoter upstream of the atpI coding sequence. Mol Gen Genet **257:** 299–307

Occhialini A, Lin MT, Andralojc PJ, Hanson MR, Parry MA (2016) Transgenic tobacco plants with improved cyanobacterial Rubisco expression but no extra assembly factors grow at near wild-type rates if provided with elevated CO_2. Plant J **85:** 148–160

Oey M, Lohse M, Kreikemeyer B, Bock R (2009a) Exhaustion of the chloroplast protein synthesis capacity by massive expression of a highly stable protein antibiotic. Plant J **57:** 436–445

Oey M, Lohse M, Scharff LB, Kreikemeyer B, Bock R (2009b) Plastid production of protein antibiotics against pneumonia via a new strategy for high-level expression of antimicrobial proteins. Proc Natl Acad Sci USA **106:** 6579–6584

Pasoreck EK, Su J, Silverman IM, Gosai SJ, Gregory BD, Yuan JS, Daniell H (2016) Terpene metabolic engineering via nuclear or chloroplast genomes profoundly and globally impacts off-target pathways through metabolite signalling. Plant Biotechnol J **14:** 1862–1875

Plader W, Sugiura M (2003) The Shine-Dalgarno-like sequence is a negative regulatory element for translation of tobacco chloroplast rps2 mRNA: An additional mechanism for translational control in chloroplasts. Plant J **34:** 377–382

Sarrion-Perdigones A, Falconi EE, Zandalinas SI, Juárez P, Fernández-del-Carmen A, Granell A, Orzaez D (2011) GoldenBraid: An iterative cloning system for standardized assembly of reusable genetic modules. PLoS ONE **6:** e21622

Schelkunov MI, Shtratnikova VY, Nuraliev MS, Selosse MA, Penin AA, Logacheva MD (2015) Exploring the limits for reduction of plastid genomes: A case study of the mycoheterotrophic orchids *Epipogium aphyllum* and *Epipogium roseum*. Genome Biol Evol **7:** 1179–1191

Schindel HS, Piatek AA, Stewart CN Jr, Lenaghan SC (2018) The plastid genome as a chassis for synthetic biology-enabled metabolic engineering: Players in gene expression. Plant Cell Rep **37:** 1419–1429

Shaver JM, Oldenburg DJ, Bendich AJ (2006) Changes in chloroplast DNA during development in tobacco, *Medicago truncatula*, pea, and maize. Planta **224:** 72–82

Shiina T, Allison L, Maliga P (1998) rbcL transcript levels in tobacco plastids are independent of light: Reduced dark transcription rate is compensated by increased mRNA stability. Plant Cell **10:** 1713–1722

Sriraman P, Silhavy D, Maliga P (1998) The phage-type PclpP-53 plastid promoter comprises sequences downstream of the transcription initiation site. Nucleic Acids Res **26:** 4874–4879

Staub JM, Maliga P (1992) Long regions of homologous DNA are incorporated into the tobacco plastid genome by transformation. Plant Cell **4:** 39–45

Staub JM, Maliga P (1994) Translation of psbA mRNA is regulated by light via the 5′-untranslated region in tobacco plastids. Plant J **6:** 547–553

Suzuki JY, Sriraman P, Svab Z, Maliga P (2003) Unique architecture of the plastid ribosomal RNA operon promoter recognized by the multisubunit RNA polymerase in tobacco and other higher plants. Plant Cell **15:** 195–205

Svab Z, Maliga P (1993) High-frequency plastid transformation in tobacco by selection for a chimeric aadA gene. Proc Natl Acad Sci USA **90:** 913–917

Tabatabaei I, Ruf S, Bock R (2017) A bifunctional aminoglycoside acetyltransferase/phosphotransferase conferring tobramycin resistance provides an efficient selectable marker for plastid transformation. Plant Mol Biol **93:** 269–281

Tanaka M, Obokata J, Chunwongse J, Shinozaki K, Sugiura M (1987) Rapid splicing and stepwise processing of a transcript from the psbB operon in tobacco chloroplasts: Determination of the intron sites in petB and petD. Mol Gen Genet **209:** 427–431

Tangphatsornruang S, Birch-Machin I, Newell CA, Gray JC (2011) The effect of different 3′ untranslated regions on the accumulation and stability of transcripts of a gfp transgene in chloroplasts of transplastomic tobacco. Plant Mol Biol **76:** 385–396

Tregoning JS, Nixon P, Kuroda H, Svab Z, Clare S, Bowe F, Fairweather N, Ytterberg J, van Wijk KJ, Dougan G, et al (2003) Expression of tetanus toxin Fragment C in tobacco chloroplasts. Nucleic Acids Res **31:** 1174–1179

Trucco V, de Breuil S, Bejerman N, Lenardon S, Giolitti F (2014) Complete nucleotide sequence of Alfalfa mosaic virus isolated from alfalfa (*Medicago sativa* L.) in Argentina. Virus Genes **48:** 562–565

Vafaee Y, Staniek A, Mancheno-Solano M, Warzecha H (2014) A modular cloning toolbox for the generation of chloroplast transformation vectors. PLoS ONE **9:** e110222

Valkov VT, Gargano D, Scotti N, Cardi T (2014) Plastid transformation in potato: *Solanum tuberosum*. Methods Mol Biol **1132:** 295–303

Verhounig A, Karcher D, Bock R (2010) Inducible gene expression from the plastid genome by a synthetic riboswitch. Proc Natl Acad Sci USA **107:** 6204–6209

Verma D, Daniell H (2007) Chloroplast vector systems for biotechnology applications. Plant Physiol **145:** 1129–1143

Verma D, Samson NP, Koya V, Daniell H (2008) A protocol for expression of foreign genes in chloroplasts. Nat Protoc **3:** 739–758

Weber E, Engler C, Gruetzner R, Werner S, Marillonnet S (2011) A modular cloning system for standardized assembly of multigene constructs. PLoS ONE **6:** e16765

Wurbs D, Ruf S, Bock R (2007) Contained metabolic engineering in tomatoes by expression of carotenoid biosynthesis genes from the plastid genome. Plant J **49:** 276–288

Xie G, Allison LA (2002) Sequences upstream of the YRTA core region are essential for transcription of the tobacco atpB NEP promoter in chloroplasts in vivo. Curr Genet **41:** 176–182

Yukawa M, Kuroda H, Sugiura M (2007) A new in vitro translation system for non-radioactive assay from tobacco chloroplasts: Effect of pre-mRNA processing on translation *in vitro*. Plant J **49:** 367–376

Zhang J, Ruf S, Hasse C, Childs L, Scharff LB, Bock R (2012) Identification of cis-elements conferring high levels of gene expression in non-green plastids. Plant J **72:** 115–128

Zhou F, Karcher D, Bock R (2007) Identification of a plastid intercistronic expression element (IEE) facilitating the expression of stable translatable monocistronic mRNAs from operons. Plant J **52:** 961–972

Zhou F, Badillo-Corona JA, Karcher D, Gonzalez-Rabade N, Piepenburg K, Borchers AM, Maloney AP, Kavanagh TA, Gray JC, Bock R (2008) High-level expression of human immunodeficiency virus antigens from the tobacco and tomato plastid genomes. Plant Biotechnol J **6:** 897–913

Zou Z, Eibl C, Koop HU (2003) The stem-loop region of the tobacco psbA 5'UTR is an important determinant of mRNA stability and translation efficiency. Mol Genet Genomics **269:** 340–349